RESEARCH PAPER

Site- and species-specific responses of forest growth to climate across the European continent

Flurin Babst[1]*, Benjamin Poulter[1,2], Valerie Trouet[3], Kun Tan[2],
Burkhard Neuwirth[4], Robert Wilson[5], Marco Carrer[6], Michael Grabner[7],
Willy Tegel[8], Tom Levanic[9], Momchil Panayotov[10], Carlo Urbinati[11],
Olivier Bouriaud[12], Philippe Ciais[2] and David Frank[1,13]

[1]*Swiss Federal Research Institute WSL, Zürcherstrasse 111, CH 8903 Birmensdorf, Switzerland, [2]Laboratoire des Sciences du Climat et de L'Environnement, CEA-CNRS-UVSQ, F-91191 Gif-sur-Yvette, France, [3]Laboratory of Tree-Ring Research, Univ. of Arizona, 105 West Stadium, Tucson, AZ 85721-0058, USA, [4]DeLaWi TreeRingAnalyses, Preschlinallee 2, D-51570 Windeck, Germany, [5]School of GeoSciences, University of Edinburgh, West Mains Road, Edinburgh EH93JW, UK, [6]Forest Ecology Research Unit, TeSAF Department, Univ. degli Studi di Padova, Agripolis, Legnaro (PD), Italy, [7]Institute of Wood Science and Technology, Universität für Bodenkultur, Gregor Mendel Strasse 33, A-1180 Vienna, Austria, [8]Institute for Forest Growth, University of Freiburg, Tennenbacherstrasse 4, 79106 Freiburg, Germany, [9]Slovenian Forestry Institute, Vecna Pot 2, 1000 Ljubljana, Slovenia, [10]Dendrology Department, University of Forestry, Sv. Kliment Ochridski 10, 1756 Sofia, Bulgaria, [11]Universita Politecnica delle Marche, Piazza Roma 22, 60121 Ancona, Italy, [12]Forest Research and Management Institute, ICAS, Sos. Stefanesti 128, O77190 Voluntari, Romania, [13]Oeschger Center for Climate Change, Zähringerstrasse 25, CH-3012 Bern, Switzerland*

*Correspondence: Flurin Babst, Zürcherstrasse 111, CH-8047 Birmensdorf, Switzerland. E-mail: flurin.babst@wsl.ch

ABSTRACT

Aim To evaluate the climate sensitivity of model-based forest productivity estimates using a continental-scale tree-ring network.

Location Europe and North Africa (30–70° N, 10° W–40° E).

Methods We compiled close to 1000 annually resolved records of radial tree growth for all major European tree species and quantified changes in growth as a function of historical climatic variation. Sites were grouped using a neural network clustering technique to isolate spatiotemporal and species-specific climate response patterns. The resulting empirical climate sensitivities were compared with the sensitivities of net primary production (NPP) estimates derived from the ORCHIDEE-FM and LPJ-wsl dynamic global vegetation models (DGVMs).

Results We found coherent biogeographic patterns in climate response that depend upon (1) phylogenetic controls and (2) ambient environmental conditions delineated by latitudinal/elevational location. Temperature controls dominate forest productivity in high-elevation and high-latitude areas whereas moisture sensitive sites are widespread at low elevation in central and southern Europe. DGVM simulations broadly reproduce the empirical patterns, but show less temperature sensitivity in the boreal zone and stronger precipitation sensitivity towards the mid-latitudes.

Main conclusions Large-scale forest productivity is driven by monthly to seasonal climate controls, but our results emphasize species-specific growth patterns under comparable environmental conditions. Furthermore, we demonstrate that carry-over effects from the previous growing season can significantly influence tree growth, particularly in areas with harsh climatic conditions – an element not considered in most current-state DGVMs. Model–data discrepancies suggest that the simulated climate sensitivity of NPP will need refinement before carbon-cycle climate feedbacks can be accurately quantified.

Keywords

Climate impacts, dendroclimatology, DGVM, forest ecology, forest productivity, LPJ, NPP, ORCHIDEE, terrestrial carbon cycle, tree-ring.

INTRODUCTION

Forests world-wide are known as an important net carbon sink and are thus a key component of the terrestrial carbon cycle. The total sink in established forests is currently estimated at 2.4 ± 0.4 Pg C year^{-1} (Pan *et al.*, 2011) and equals approximately 25% of the current global anthropogenic fossil fuel emissions (Friedlingstein *et al.*, 2010). However, carbon fluxes and storage vary regionally and with interannual to long-term environmental change (Luyssaert *et al.*, 2010). For example, it was estimated

that the 2003 summer drought in Europe caused a 30% reduction in continental-scale net primary productivity (NPP), temporarily turning terrestrial ecosystems into a net carbon source (Ciais *et al.*, 2005). The impacts of this heatwave were spatially variable, particularly in regions characterized by complex topography. In the Swiss Alps for instance, increased productivity of the subalpine forests due to lengthening of the growing season was contrasted by decreased growth at lower elevations due to drought stress (Jolly *et al.*, 2005). A higher frequency of drought events and other negative impacts on growth (increased autotrophic respiration and disturbances) are predicted to outweigh enhanced productivity due to increasing temperatures (Hoch & Körner, 2012) or CO_2 and nitrogen fertilization (Sitch *et al.*, 2008). If this is correct, then future reductions in forest CO_2 uptake will have profound implications for the terrestrial carbon cycle and related climate feedbacks (Frank *et al.*, 2010), as well as for species distribution ranges (Hickler *et al.*, 2012) and forest management practices.

Considerable observational and modelling efforts have been invested to better constrain climate-induced changes in carbon pools. Global NPP was recently indicated to have decreased by 0.55 Pg C between 2000 and 2009, but when looked at in detail it is apparent that this reduction was driven by increased Southern Hemisphere drought which outweighed a warming-induced productivity increase in the northern boreal and temperate zones (Zhao & Running, 2010). NPP trends even differ strongly on a subcontinental scale, and estimates based on current-state vegetation models are subject to considerable uncertainty. Exact estimation of forest productivity is currently hampered by our limited understanding of the climatic drivers of wood formation as a function of species, ecological conditions and geographic location (Stegen *et al.*, 2011). As a consequence, uncertainties in interannual to long-term variability in tree growth will continue to challenge large-scale NPP simulations until its climatic drivers are well understood.

Annual radial growth increment, i.e. tree-ring width, is an important parameter that allows tree growth and climate variability to be connected on local to continental scales. Radial growth data from increment cores are shown to be broadly compatible with productivity estimates from forest inventory data (Metsaranta & Lieffers, 2009), eddy-covariance measurements (Zweifel *et al.*, 2010) and carbon budget models (Metsaranta & Kurz, 2012); however, the suitability of tree-rings to serve as a direct proxy for ecosystem productivity has not yet been fully tested. Recent studies have shown growth to be highly correlated at different stem heights (van der Maaten-Theunissen & Bouriaud, 2012), demonstrating that cores taken from near the stem base are tightly linked with both total stem productivity and stand-level NPP (Bouriaud *et al.*, 2005). Numerous dendroclimatological studies have provided insights in the influence of tree age (Esper *et al.*, 2008), altitude (Levanic *et al.*, 2009) and site ecology (Neuwirth *et al.*, 2004) on the climate sensitivity of tree growth. Furthermore, the establishment of regional-scale networks allowed the spatial and species-specific growth response patterns to be connected with thermal and moisture variations within particular climatic zones (Frank & Esper, 2005;

Büntgen *et al.*, 2007; Friedrichs *et al.*, 2009; Affolter *et al.*, 2010). Only a few studies, however, have addressed large-scale climate responses of forests in Europe (Briffa *et al.*, 2002; Wettstein *et al.*, 2011). These studies did not resolve topographic and species-specific characteristics and therefore are not adequate for the validation and improvement of vegetation and carbon cycle models. Thus, a well-replicated, continental scale assessment of the climate response of forests is needed to: (1) determine the temporal and spatial scales at which climate limits tree growth, (2) quantify the sensitivity of growth to changes in climate, and (3) test if vegetation models correctly handle the response of NPP to climate variability.

Here, we perform a Europe-wide analysis of tree growth response patterns based on tree-ring data and modelled NPP from two process-based dynamic global vegetation models (DGVMs). We compiled chronologies from 36 coniferous and broadleaf species to assess the climate forcing of radial tree growth. A nonlinear classification approach known as self-organizing maps (SOMs) was applied to group sites with similar climate responses. These site groups were then assessed to detect first-order patterns in climate forcing as a function of: (1) geographic position, (2) mean climatology and (3) tree species. In addition to the empirical growth quantification, monthly NPP was estimated using two process-based DGVMs (ORCHIDEE-FM, LPJ-wsl). As a first test to evaluate DGVMs with tree-ring networks, correlation analyses were used to compare the spatial distribution and magnitude of climate sensitivity of modelled NPP to the patterns suggested by annually resolved tree-ring data.

DATA AND METHODS

Tree-ring network

We compiled tree-ring width (TRW) information from approximately 1000 sites into a dataset covering most of Europe and parts of North Africa (30–70° N/10° W–40° E), with sites ranging from sea level to 2500 m a.s.l. in Mediterranean mountain ranges (Fig. 1a). Standardized data are provided in Appendices S3 and S4 in Supporting Information. Prior analyses on portions of this dataset including the greater Alpine region (Frank & Esper, 2005), central Germany (Friedrichs *et al.*, 2009), the Tatra Mountains (Büntgen *et al.*, 2007), the Scottish Highlands (Wilson *et al.*, 2012), the Pirin Mountains (Panayotov *et al.*, 2010), the eastern Alps (Levanic *et al.*, 2009), northeastern France (Tegel *et al.*, 2010), the Apennines (Carrer *et al.*, 2010), central (Neuwirth *et al.*, 2004) and northern Europe (e.g. Gouirand *et al.*, 2008) have generally been directed at quantifying local to regional growth variability.

The network contains 36 tree species, the most common of which are shown in Fig. 1(b). We will subsequently use the following abbreviations: PCAB (*Picea abies*), PISY (*Pinus sylvestris*), ABAL (*Abies alba*), LADE (*Larix decidua*), PICE (*Pinus cembra*), FASY (*Fagus sylvatica*), QURO (*Quercus robur*), QUPE (*Quercus petraea*). Less frequently represented species are combined under the 'other conifers' and 'other broadleaf' categories.
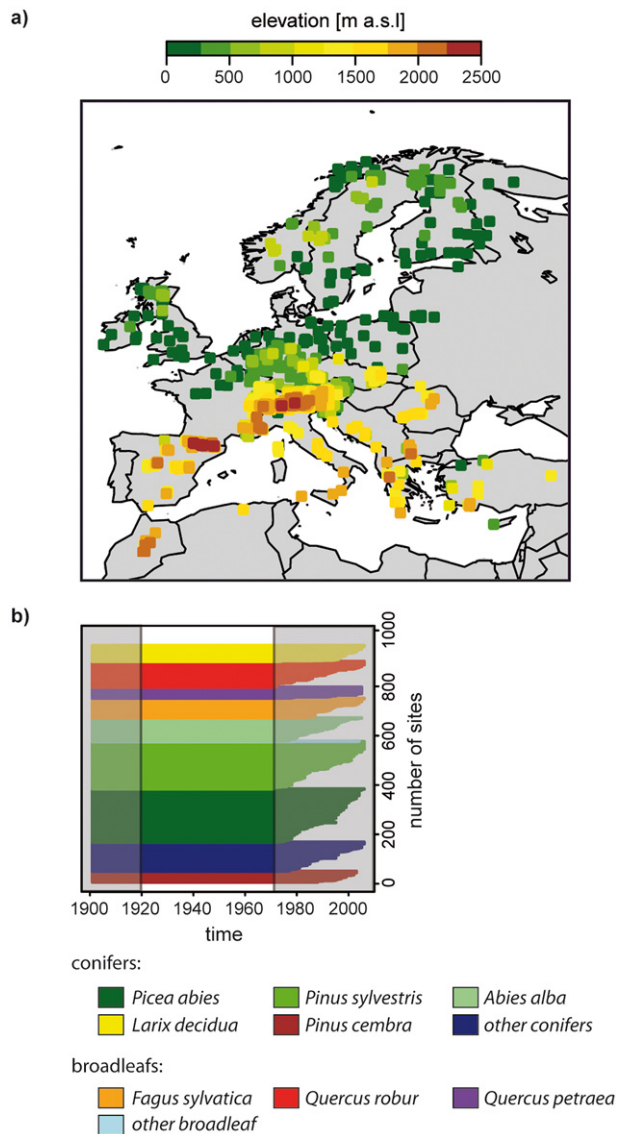
Figure 1 Tree-ring network containing ring-width chronologies from 992 sites across Europe. (a) Geographic location and elevation of each site as well as (b) the replication of the eight most frequent tree species over time are presented. Further species contained in the network are categorized as 'other conifers' and 'other broadleaf'. All analyses focus on the time window between 1920 and 1970. Map area: 30–70° N, 10° W–40° E.

To investigate the effect of climate forcing on radial tree growth, it is necessary to remove the biological age trend that is present in raw TRW measurement series (e.g. Esper *et al.*, 2002). This was accomplished using a spline with a 50% frequency cutoff response at 32 years. Our choice of detrending will remove most of the variance related to multidecadal or longer-term climatic trends, and this study will thus focus on interannual to decadal variability. Removing the age-related trend with a 300-year spline, and thus preserving more low-frequency variability, did not significantly alter the strength or patterns of climate response. Prior to detrending, the heteroscedastic variance structure related to the age trend was stabilized using an

adaptive power transformation (Cook & Peters, 1997) before calculating residuals from detrending functions. This procedure introduces a nonlinear transformation that may be relevant for the quantification of climate sensitivities. Tests on a random network subset, however, demonstrated that the impact of variance stabilization on TRW correlations with climate data is negligible (Appendix S2 and Fig. S1).

To ensure a certain degree of robustness in our growth–climate analyses, site chronologies were required to meet the following criteria: (1) sample replication at site level was greater than five series and the expressed population signal (EPS) of the chronologies was above 0.85 (Wigley *et al.*, 1984); (2) the period 1920–70 was entirely covered by the time series to ensure sufficient overlap with instrumental measurements.

A total of 992 sites were retained for final analysis, making this the most comprehensive investigation of climate forcing on tree growth.

Climate data

A downscaled climatology was employed to consider topographic effects on local climate. We used the gridded 0.5° × 0.5°CRU TS 3.0 global temperature and precipitation datasets (Mitchell & Jones, 2005) as a basis and downscaled them to 1-km spatial resolution using the WorldClim database of climate normals based upon the GTOPO30 digital elevation model (Hijmans *et al.*, 2005). For temperature, absolute anomalies were calculated by subtracting the long-term (1950–2000, corresponding to WorldClim) monthly means from the entire CRU TS 3.0 time series (1901–2005) and relative anomalies were calculated for precipitation (observed precipitation divided by monthly means). The monthly anomalies were then bilinearly interpolated to 1-km resolution and added to (or multiplied by in the case of precipitation) the WorldClim baseline climatology. Additional analyses were also performed with the gridded self-calibrating Palmer drought severity index data (scPDSI; van der Schrier *et al.*, 2006) at 0.5° resolution.

Geographic coordinates associated with tree-ring sites were sometimes coarse (e.g. 0.5° precision), leading to a mismatch in the elevations of metadata and respective WorldClim grid cells in mountainous areas. To minimize these altitudinal (and implied climate) deviations, climate data from the closest grid cell with a matching elevation were assigned to each tree-ring site. This procedure was chosen because the altitudinal precision recorded in the tree-ring metadata was often greater than the geographic precision. In most cases a suitable grid point was located within a few kilometres of the indicated site position.

Climate forcing of tree growth

The current study is a continental-scale approach dealing with multiple species and thus a great variety of growth conditions, site ecologies and growing season lengths. To address the resulting heterogeneity in climate responses, we based analyses on monthly resolved climate correlation functions (CCFs) between TRW indices and temperature and precipitation (Cook *et al.*,

2001). scPDSI was not included in this analysis because this parameter shows only limited seasonality when correlated with tree-ring data (St George et al., 2010). CCFs were computed for all months starting in April of the year prior to growth (pApr) and ending in current-year September for the period 1920–70. In addition, we performed a linear regression analysis between correlations and slopes (representing sensitivity per se) of TRW indices versus summer climate at each site. The strong relationships we found for temperature ($r^2 = 0.64$) and precipitation ($r^2 = 0.86$) suggest that the correlation coefficient is closely related to climate sensitivity, and can thus be used to characterize the association strength between climate variables and TRW, even if site-level data currently prohibit an absolute (e.g. kg m^{-2} °C^{-1}) sensitivity estimation.

Self-organizing maps

To cluster the 992 sites according to their climatic drivers, we computed SOMs – an ideal method to visualize complex relationships in large datasets (Hewitson & Crane, 2002). Sites were grouped based on the temperature and precipitation CCFs for each site. SOMs are arrays of definable size with each element or 'node' representing a reference vector. These nodes are iteratively adjusted as a function of the minimal Euclidean distance to best represent the dataset's variance (Hewitson & Crane, 2002). The number of nodes chosen is a balance between a large within-node variance (few clusters) and a loss of generalization (many clusters; Trouet et al., 2006). We selected a 3 × 3 node array, where the nine reference vectors can be interpreted as the general climate response patterns of all sites within the particular clusters. Within the SOM array, nodes are arranged in such a way that the most unequal response types are placed in opposing corners. This enables an interpretation of the clusters towards temperature, precipitation and mixed sensitivity.

Modelled net primary productivity (NPP)

We performed correlation and linear regression analyses between model-based NPP estimates and climate data at each of the 992 sites and compared the results with tree-ring derived climate sensitivities. Monthly NPP was computed using two different process-based dynamic global vegetation models (DGVMs) ORCHIDEE-FM (ORC; Bellassen et al., 2010) and LPJ-wsl (Poulter et al., 2011). NPP estimates from both DGVMs are provided in Appendices S5 and S6. A description of model runs, input data and differences in model structures is provided in Appendix S1. We calculated summer and annual NPP as the site-specific productivity averaged over three (June–August; JJA) and 12 (January–December) months, respectively. JJA climate represents the strongest common driver of TRW in Europe, despite the longer growing season at temperate and larger growth in spring and autumn at Mediterranean sites with dry summers (Briffa et al., 2002). Furthermore, the summer season may exclude biases in cold months when respiration may over-compensate GPP leading to negative productivity estimates (Piao et al., 2009).

RESULTS

Monthly and seasonal climate response

The climate response of tree-ring width (TRW) chronologies was assessed over two growing seasons including the winter in between. Figure 2 provides a broad spatial overview of the climate sensitivities (mean JJA temperatures, precipitation sums and scPDSI values), and species-specific monthly climate response patterns are shown in Fig. S2 (Appendix S2). The strongest positive relationships between TRW and temperature ($r > 0.6$) occur in cold and humid areas, such as the Scandes mountain range, northernmost Great Britain, the central Alpine tree line, and the Dinaric Mountains (Fig. 2). In similarly cool but drier areas (e.g. eastern Scandinavia, high-elevation Alpine valleys, the Pyrenees, and Mediterranean tree-line sites), temperature correlation coefficients decrease to 0.4–0.6 or less. Trees in temperate and Mediterranean lowland regions generally revealed no distinct thermal signal. Negative correlations between TRW and JJA temperature occur mainly around the eastern part of the Mediterranean Sea and in northern Africa. Sporadically, negative correlations with temperatures were also observed at dry sites in the mid-latitudes, located in the rain shadow of mountain ranges such as the Vosges, the Bavarian Forest and in inner-Alpine dry valleys.

The spatial distribution of precipitation signals is more diffuse and correlation coefficients are generally lower ($r = 0.2$–0.4; Fig. 2). Positive JJA correlations were found in the central European lowlands, southern Great Britain, the Iberian Peninsula as well as in Anatolia and northernmost Africa. Strongly responsive sites ($r > 0.4$) are scarce and located at the bottom of Alpine dry valleys and in central Germany, as well as in the lee of the Alps and the northern Scandes. Pronounced negative correlations with JJA precipitation were found in the Dinaric Mountains and along the central and western Scandes.

Drought stress, integrating both evaporative demand and water availability, was assessed through correlations with scPDSI, and was shown to strongly influence many sites where positive temperature responses were not found. The distribution of scPDSI sensitive sites is comparable to the pattern revealed by precipitation-positive correlations but the signal is often considerably stronger ($r > 0.4$–0.6). The highest correlations were obtained in central Germany, France, Anatolia and northernmost Africa. Sites in southern Great Britain, south-western Finland and on the Iberian Peninsula also responded positively to scPDSI.

Climate response patterns (SOMs)

The seasonality in the climate responses of European trees varies considerably with species as well as geographic location and we therefore computed SOMs to identify broad patterns within the network. Resulting SOM nodes were grouped into three response categories based on the interpretation of the average CCF of each node and the arrangement of the nodes in the SOM array (Fig. 3a): 'temperature signal' (N2, N3 and N6), 'precipitation signal' (N4, N7 and N8) and 'mixed signal' (N1, N5 and
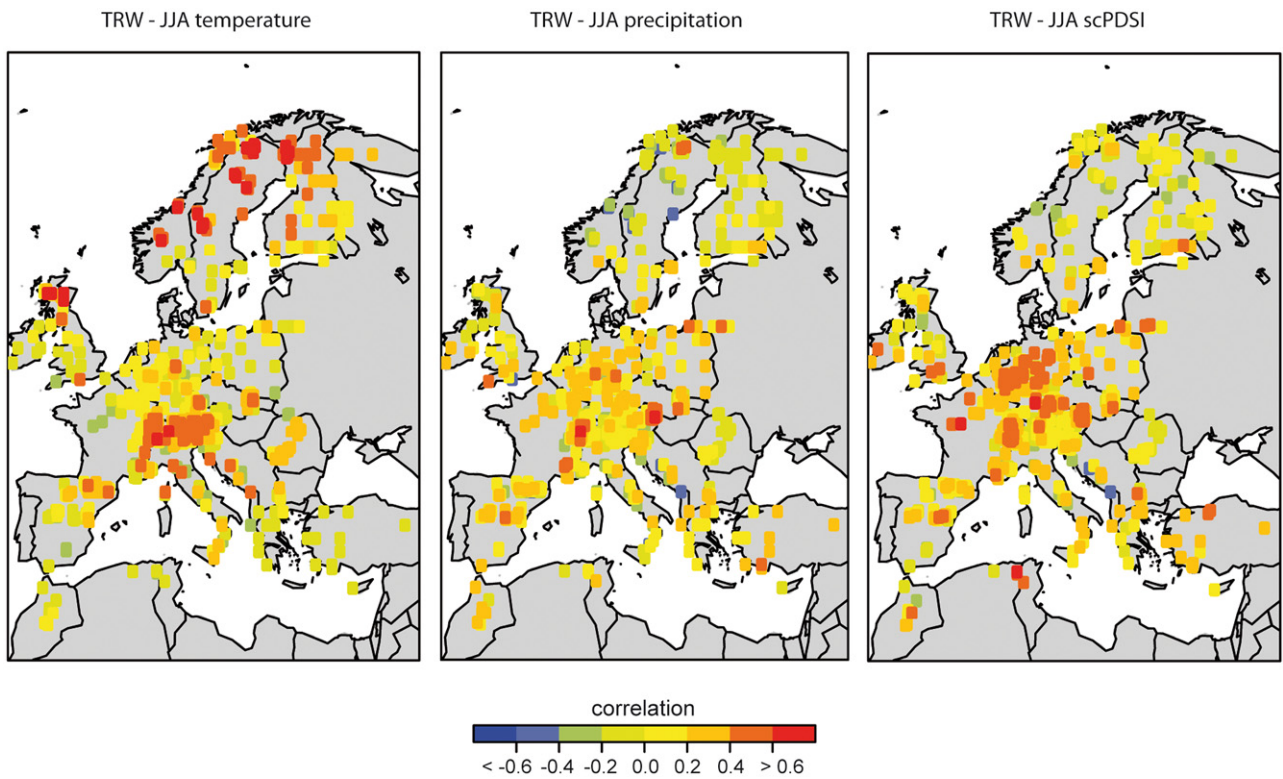
Figure 2 Correlations between tree-ring width (TRW) and current year June–August (JJA) temperature means (left), cumulative June–August precipitation amounts (middle) as well as the self-calibrating Palmer drought severity index (scPDSI, right). Map area: 30–70° N, 10° W–40° E.
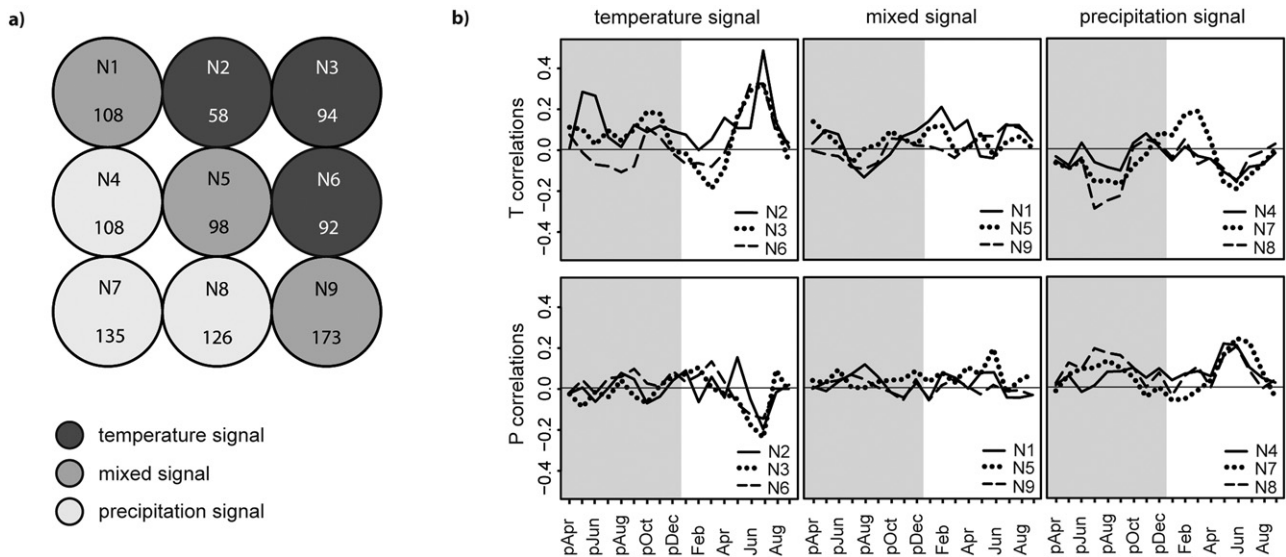
Figure 3 Nine nodes (clusters N1–N9) derived from the self-organizing maps (SOMs) algorithm applied to monthly climate correlations with radial growth at all sites in the tree-ring network. (a) The classification of nodes in the SOM array according to temperature, precipitation and mixed sensitivity is shown. Additionally, the number of sites compiled in each node is indicated. (b) Correlations between average radial growth of each node and mean monthly temperature (top) and precipitation (bottom) are presented for the previous (pApr to pDec, shaded in grey) and current growing seasons. Nodes have been grouped according to their climate sensitivity.

N9). A plot of the three average CCFs of the three nodes in each response category enables a direct comparison of response types (Fig. 3b). Temperature-sensitive nodes commonly responded to current summer climate and internode differences were introduced by temperature responses during preceding seasons. TRW at precipitation-sensitive sites responded moderately positively to precipitation during most months, with peaks in the current summer for all three nodes and in the previous summer for N7 and N8. Negative correlations with summer temperature at these sites are a further indicator of the importance of drought stress. Mixed signal nodes generally did not show pronounced responses to individual climate parameters and correlations with temperature and precipitation were generally low.

Detailed information about seasonal and species-specific climate response patterns are revealed by the individual nodes belonging to the three signal categories (Fig. 4). Temperature-sensitive sites are characterized by positive reactions to summer temperatures (July in N2, June/July in N3 and N6) and negative responses to summer precipitation (July in N2 and N3, May–July in N6). N2 is dominated by PISY stands in northern Scandinavia, N3 contains Alpine tree line sites composed of PICE and LADE, and N6 consists almost exclusively of PCAB in the Alps, the Tatra Mountains, the Bavarian Forest, and central to northern Scandinavia. Lag effects from prior May/June temperature influence TRW at N2 sites, whereas high early spring temperatures negatively influence growth at N3 stands. Furthermore, October thermal conditions of the previous year positively affect TRW at N6.

Sites with a positive precipitation response are clustered in nodes 4, 7 and 8 (Fig. 4b). N4 represents lowland oak (QURO/QUPE) in central and south-eastern Europe, France and southern Great Britain. Some dry PISY stands in the Alpine arc show a similar response pattern. Positive correlations with precipitation occur in May/June whereas no distinct reaction to temperature is visible. N7 primarily consists of Mediterranean pine sites as well as low-elevation ABAL stands in Italy and PCAB in south-eastern Germany. At these dry sites, growth is positively correlated with precipitation and negatively with temperature during May–July. Furthermore, high winter (January–March) temperatures facilitate growth. N8 is moderately sensitive to May/June as well as to previous July–September precipitation. Also, these FASY (central Germany) and PCAB (lower Alps) sites correlate negatively with previous summer temperature.

Mixed signal sites are compiled in nodes 1, 5 and 9 (Fig. 4c). N1 combines ABAL in central Europe with PISY in southern Scandinavia and northern Great Britain. N5 contains most of the QURO sites in central Europe that do not fall into N4. All remaining chronologies, mainly mid-elevation PCAB in the Alps/Carpathians and PISY in southern Scandinavia and northern Great Britain, are compiled in N9.

Latitudinal/altitudinal distribution of climate signals

From the above analysis, it is clear that species and geographic position influence response to climate. The maps in Fig. 4, however, do not allow assessments of climate variation associated with elevation gradients. We therefore plotted the three climate response categories in latitudinal and altitudinal space over Europe (Fig. 5a). A distinct separation of precipitation- and temperature-limited sites is apparent and mixed signal stands are mostly situated along or near this boundary zone. The dividing boundary has a negative exponential shape starting at tree line (2250 m a.s.l.) at around 42° N, descending to 1000 m a.s.l. at 49° N, and approaching sea level above 60° N latitude. For verification, a SOM-independent assessment of the geographic location of climate-responsive ($r > 0.3$ to seasonal precipitation or temperature; Fig. 5b) sites shows a similar spatial distribution for June–August and April–September climate. Other seasons are less well represented, yet reinforce the above findings for continental to subregional patterns in the climatic drivers of forest productivity.

Climate sensitivity of model-based NPP estimates

The empirical analysis of the climate dependency of radial growth across Europe presents an interesting opportunity to benchmark and evaluate the ORC and LPJ NPP simulations. We find that ORC performs slightly better in reproducing the positive summer (Fig. 6) and annual (Appendix S2, Fig. S3) temperature responses found in the tree-ring network. However, in Central Europe and the Mediterranean region, ORC NPP is negatively correlated ($r < −0.4$) with temperature and simultaneously positively and strongly correlated ($r > 0.4$) with summer precipitation. LPJ NPP values on the other hand are strongly negatively correlated with summer temperature in southern Fennoscandia ($r < −0.4$) and moderately negatively correlated in central Europe and the Mediterranean area ($r = −0.2$ to $−0.4$). Furthermore, LPJ results are most precipitation sensitive in southern Europe ($r > 0.6$) and southern Scandinavia ($r = 0.2$–0.4). These relationships among the climate sensitivities of the two DGVMs and comparisons with the tree-ring network are confirmed by the regression analyses and contour plots shown in Fig. 6 (insets). The correspondence to the empirical tree-ring data is slightly stronger for ORC NPP, but both models show a lower temperature sensitivity in Scandinavia and generally higher precipitation sensitivities than tree rings. The strong positive temperature response of LPJ in the Alps (cold and humid) and very low correlations in northern Scandinavia (cold and dry) is further indicative of a stronger drought sensitivity compared with tree rings. The same effect is to a lesser extent visible in ORC and confirmed by high correlations with summer precipitation in the Mediterranean and central Europe. NPP shown in Fig. 6 was calculated using the FAO soil input data (Zobler, 1986), which is likely to be consistent with the parameterization for drought stress in both DGVMs. More extreme European-wide drought stress is suggested when simulations are driven using the shallower JRC soil dataset (see Appendix S2, Fig. S4).

DISCUSSION AND CONCLUSIONS

We established an extensive network of TRW data over Europe to assess growth–climate relationships on a continental scale. Our results reveal consistent climate response patterns that help

F. Babst *et al.*
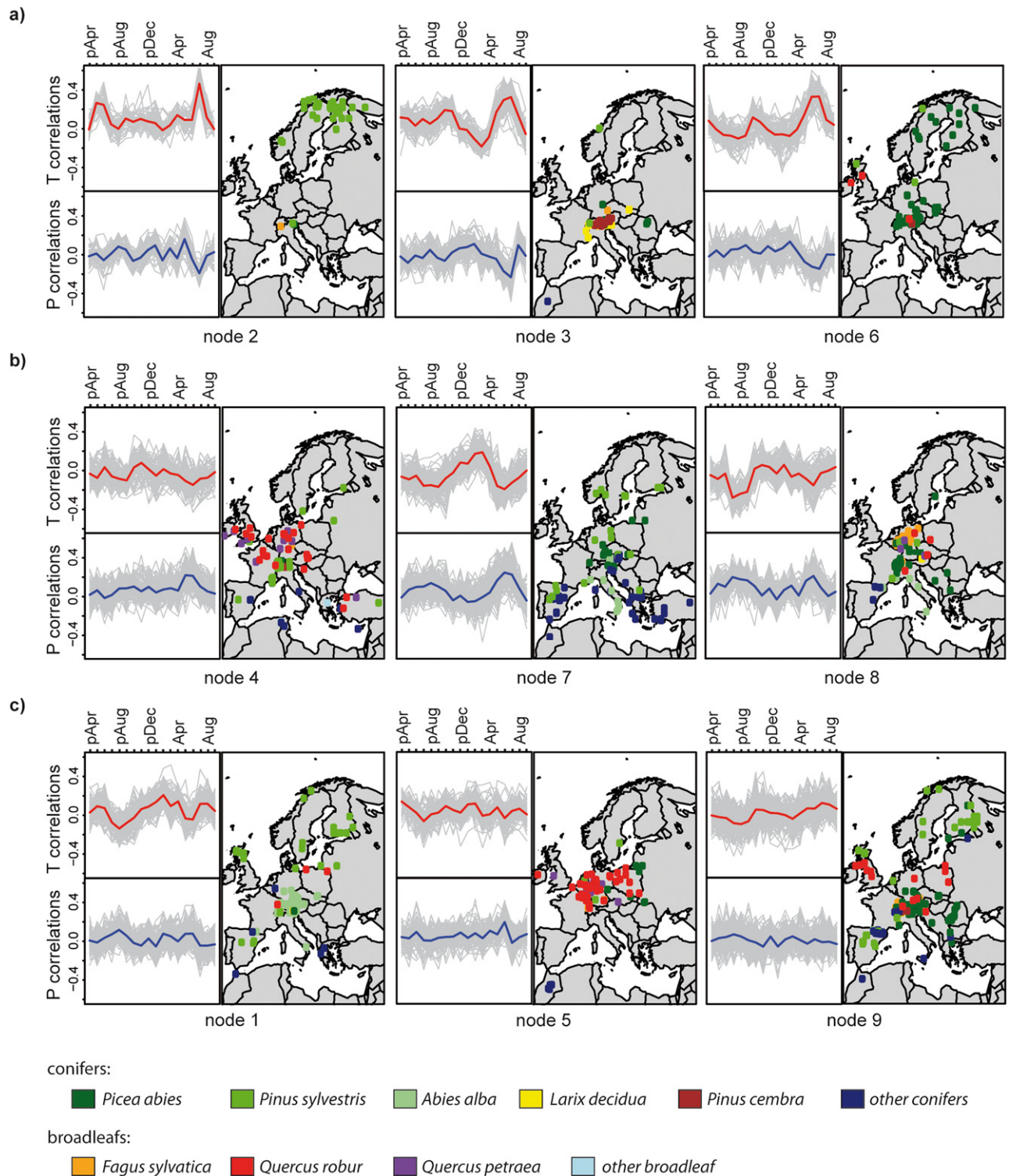
Figure 4 Spatial distribution of the nine nodes over Europe based on self-organizing maps (SOMs). The colours represent the most frequent conifer and broadleaf species. Additionally, the correlations with monthly temperature (top, mean displayed in red) and precipitation (bottom, mean displayed in blue) at each site are shown between April of the year prior to ring development (pApr) and the current September. Nodes are arranged according to (a) temperature, (b) precipitation and (c) mixed sensitivity as classified in the SOM array (Fig. 3a). Map area: 30–70° N, 10° W–40° E.
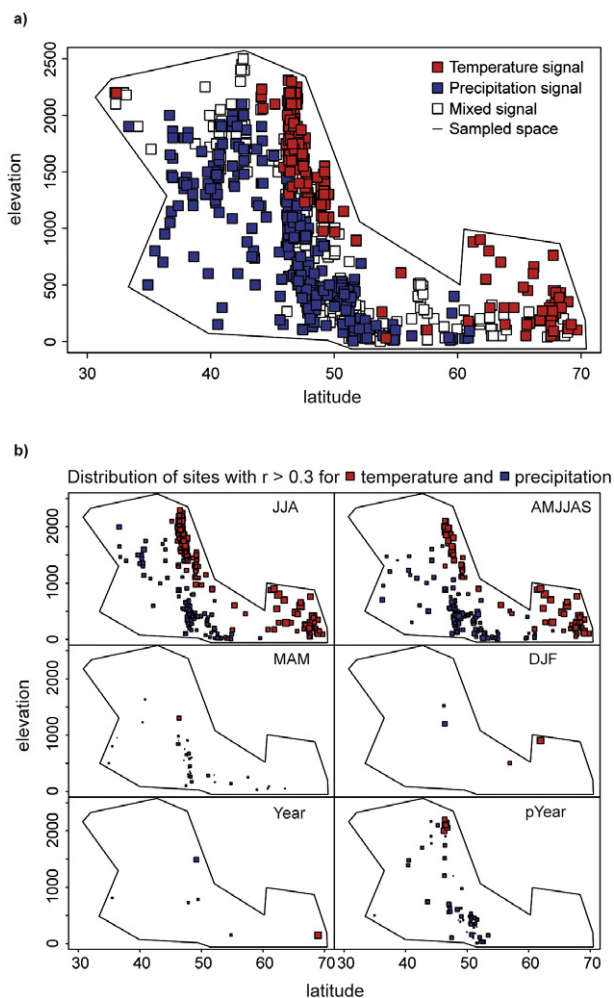
Figure 5 Distribution of temperature and precipitation signals in altitudinal and latitudinal space across Europe. The black polygons represent the total sampled area. The top figure (a) shows the distribution based on a self-organizing map (SOM) classification, the bottom figures (b) display responsive sites ($r > 0.3$) for six different seasons (letters correspond to sequential months, pYear is the year prior to ring development). Symbol sizes correspond to signal strength.

evaluate the accuracy of spatiotemporal variability in NPP simulation from DGVMs. However, it is important to note that this tree-ring compilation consists of data that were collected by a variety of researchers, for numerous investigations with differing sampling designs. While the sampled space, sites and species cannot be considered to be fully representative of European forests, we were nevertheless able to identify broad geographic, climatic and species-specific controls on tree growth across the continent.

Analyses of annual growth response to summer temperature largely reflect the 'common knowledge' of distinct temperature signals at high elevations and latitudes (Fritts, 1976). However, even in characteristically cold regions where temperature would be expected to be the single dominant factor, correlation coefficients decrease with reduced water availability. In the Alps, this is

the case in dry valleys (e.g. Affolter et al., 2010), whereas in Scandinavia, temperature responses decrease with the moisture gradient from the maritime west to the more continental east, reinforcing the findings of Helama et al. (2005) who assessed the climate response of forests across Finland. The spatial distribution of sites that respond to summer precipitation and scPDSI is more diffuse and strongly related to topography. Signals from the scPDSI, a measure of soil moisture and thus a better estimate of the water available for trees (Cook et al., 2010), are considerably stronger than those from precipitation. Yet, monthly climate responses (Appendix S2, Fig. S2) suggest that European forest growth is not driven by climate during a single time-window. Instead we observed a diverse seasonality that can be explained by differing growing season lengths (Moser et al., 2010), emergent manifestations of complex tree physiological processes (Cook & Pederson, 2011), lag effects from the previous year (Frank & Esper, 2005), as well as site properties. This finding is likely to have important implications for tree-ring based spatial climate reconstructions (e.g. Briffa et al., 2002) which usually focus on one specific season (St George et al., 2010).

We found SOM models to be an ideal tool for assessing patterns of common variances in extensive tree-ring networks, because the corners of the 3×3 node array can be interpreted as the most unequal climate response types whereas neighbouring nodes react to similar drivers. Assigning sites to climate signal categories in this way may occasionally result in a classification differing from a single-monthly or seasonal classification. For instance, in northern Great Britain, PISY sites often show a moderate summer temperature signal (Wilson et al., 2012; Fig. 2) whereas their overall response is assigned to a mixed signal node (Fig. 4c).

An essential result of our SOM analysis is the grouping of species from diverse geographic regions and the separation of confined regions by species solely based on their climate response functions (e.g. PISY and PCAB in Fennoscandia; Fig. 4a). Such a separation underlines the importance of species-specific growth responses compared to common environmental drivers. This has implications for the use of generic plant functional types (e.g. Jung et al., 2007) in DGVMs to compute forest productivity. Refinement of the species types by including their characteristic climate responses could potentially improve regional estimates of the response of NPP to climate variability and change, as well as estimates of competitive success and thus future biodiversity.

Growth at temperature- or precipitation-sensitive sites generally responds to current summer climate. Thus, the separation of nodes is largely based on conditions in the period prior to the main growing season and the interpretation of node differences is closely related to geographic location and topography. For instance, Alpine tree line species in N3 respond negatively to high previous winter temperatures which are associated with increased respiratory carbon costs (Piao et al., 2009). Other sites are positively influenced by previous summer (N2 and N8) and autumn (N6) climate. Such lag effects are possibly introduced by enhanced nutrient storage and a variety of climate and biological processes such as a delayed end of the growing season (Moser
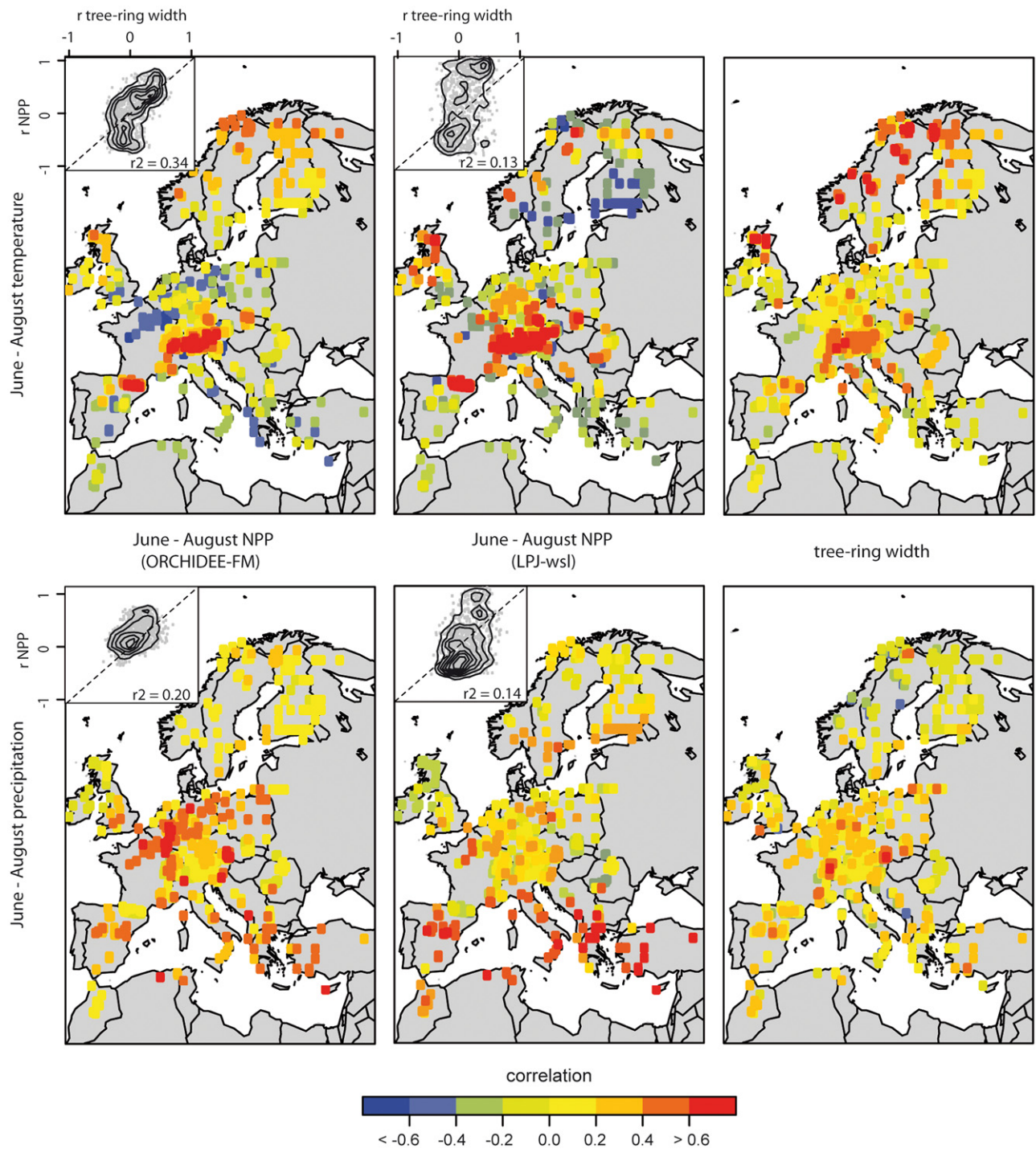
Figure 6 Comparison of the June to August climate responses of empirical tree-ring data and simulated net primary productivity (NPP) derived from two dynamic global vegetation models. Correlations with temperature (top) and precipitation (bottom) are shown for NPP from ORCHIDEE-FM (left), LPJ-wsl (middle) and tree-ring width (right). NPP was estimated using FAO soil input data. The contour plot insets show direct comparisons and linear regression coefficients between the climate sensitivity of tree-ring width (horizontal axis) and modelled NPP (vertical axis) with the dashed line representing the one-to-one (target) relationship. Map area: 30–70° N, 10° W–40° E.

et al., 2010) or water availability after snow melt. Trees at moisture-limited sites generally show less seasonality in their climate response than thermally limited stands. A weak but continuously positive precipitation signal peaking in current and previous summer is commonly observed. This response pattern

explains the diffuse spatial distribution of sites that respond to summer drought. Of all moisture sensitive nodes, conifers in N7 exhibit the most pronounced seasonality and have often been used for drought reconstructions in the past (e.g. Nicault *et al.*, 2008). In latitudinal and altitudinal space, we find a surprisingly

distinct threshold between temperature- and moisture-sensitive areas. Such a distribution was postulated by Fritts (1976) but has not been empirically defined on a continental scale. Our network thus enables us for the first time to estimate the climate response of European forests as a function of elevation and latitude.

Our analyses of NPP climate response revealed clear differences between the two DGVMs, probably contributing to differences in model estimates of carbon-cycle climate feedbacks (Frank *et al.*, 2010). Comparisons with a continental-scale tree-ring network opens possibilities for a novel concept to validate, falsify and improve DGVM estimates, and should encourage further use of tree rings for model evaluation. ORC and LPJ in their current configurations are variably successful in reproducing the empirical tree-ring based climate response in different parts of Europe. Observed differences between the two models may be introduced by varying treatment of water-stressed conductance, autotrophic respiration and phenology (Sitch *et al.*, 2008). ORC is highly sensitive to summer precipitation, yet captures the general spatial variability in summer climate sensitivity of European forests. LPJ simulations exhibit an even stronger drought response, particularly in Scandinavia and the Mediterranean area, which introduces differences in NPP estimates compared to ORC and even stronger differences compared to TRW. The drought response of simulated NPP is possibly enhanced by model assumptions that do not capture the full autocorrelation effects which are often found in tree rings as a result of local water and nutrient storage or recovery after disturbance (Fritts, 1976). Our results emphasize the importance of climate conditions during the previous year for current growth performance, an issue that ought to be included in vegetation models (McDowell *et al.*, 2011). Except for possible soil moisture deficit legacies from the previous year, the models contain insufficient reserves from the prior growing season affecting allocation to wood in the following year. Additionally, none of the models include a parameterization of wood growth during a well-defined interval of the year, so that NPP is seasonally very similar to GPP.

Analyses of observed and simulated climate sensitivities revealed regional differences and identified potential for future improvement of model structures. Yet multiple factors may complicate the joint assessment of empirical TRW and simulated NPP. For instance, model simulations are forced by the same gridded historical climate data that are used for the climate response analysis. NPP correlations with climate data could thus be stronger due to such dependence on the model input. Additionally, our results suggest that the success of the models in reproducing observed climate sensitivities varies regionally while the average climate response over the entire continent is similar to TRW (Fig. S5, Appendix S2), thus emphasizing the need to carefully assess regional productivity. Climate on the other hand, is a principal but not the only driver of tree growth with site- and species-specific properties (e.g. Frank & Esper, 2005), disturbances (e.g. Babst *et al.*, 2010) and human management (Fritts, 1976) co-determining forest productivity. These additional drivers may reduce the strength of the climate signal in tree-ring data and until such factors are routinely implemented in model simulations we will have to settle for less than

optimal comparisons of modelled versus observational output. Despite the above challenges that may tend to enhance the climate response of the models in comparison to the empirical data, in our study we were still able to provide concrete evidence on model biases. For example, in Scandinavia we find a higher temperature sensitivity of TRW in comparison with NPP from both models, despite the noise contained in tree-ring data (Frank *et al.*, 2007) and the strength of the temperature signal in the model simulations. This result suggests that the above caveats do not invalidate the use of tree-rings for model evaluation and calibration and we believe that more work in this direction will prove to be quite fruitful.

This study identifies the principal climatic drivers of European forest growth, but an absolute quantification of annual biomass increment based on the currently existing tree-ring data is impractical due to lack of site control, limited meta-data availability and diverse sampling strategies. Empirical forest productivity measurements nevertheless carry a great potential to quantify the impacts of climate change on the terrestrial carbon cycle and tree-ring based DGVM validation. An adapted sampling scheme (Babst *et al.*, 2012) consistently applied on a large scale is thus required to enable absolute and annually resolved measurements of tree growth. Related assessments of coherent growth patterns, extremes and long-term trends will further contribute to improved understanding of forest carbon sink dynamics. Such work is time- and cost-intensive, but crucial for different research communities, forest management practices and for determining and implementing effective environmental policies.

REFERENCES

Affolter, P., Büntgen, U., Esper, J., Rigling, A., Weber, P., Luterbacher, J. & Frank, D.C. (2010) Inner Alpine conifer response to 20th century drought swings. *European Journal of Forest Research*, **129**, 289–298.

Babst, F., Esper, J. & Parlow, E. (2010) Landsat TM/ETM+ and tree-ring based assessment of spatiotemporal patterns of the autumnal moth (*Epirrita autumnata*) in northernmost Fennoscandia. *Remote Sensing of Environment*, **114**, 637–646.

Babst, F., Bouriaud, O. & Frank, D.C. (2012) A new sampling strategy for tree-ring based forest productivity estimates. *ATR TRACE Proceedings*, **10**, 62–70.

Bellassen, V., LeMaire, G., Dhôte, J., Ciais, P. & Viovy, N. (2010) Modelling forest management within a global vegetation

model Part 1: model structure and general behaviour. *Ecological Modelling*, **221**, 2458–2474.

Bouriaud, O., Breda, N., Dupouey, J. & Granier, A. (2005) Is ring width a reliable proxy for stem-biomass increment? A case study in European beech. *Canadian Journal of Forest Research*, **35**, 2920–2933.

Briffa, K.R., Osborn, T.J., Schweingruber, F.H., Jones, P.D., Shiyatov, S.G. & Vaganov, E.A. (2002) Tree-ring width and density data around the Northern Hemisphere: part 1, local and regional climate signals. *The Holocene*, **12**, 737–757.

Büntgen, U., Frank, D.C., Kaczka, R.J., Verstege, A., Zwijacz-Kozica, T. & Esper, J. (2007) Growth responses to climate in a multi-species tree-ring network in the western Carpathian Tatra Mountains, Poland and Slovakia. *Tree Physiology*, **27**, 689–702.

Carrer, M., Nola, P., Motta, R. & Urbinati, C. (2010) Contrasting tree-ring growth to climate responses of *Abies alba* toward the southern limit of its distribution area. *Oikos*, **119**, 1515–1525.

Ciais, P., Reichstein, M., Viovy, N. *et al.* (2005) Europe-wide reduction in primary productivity caused by the heat and drought in 2003. *Nature*, **437**, 529–533.

Cook, E.R. & Pederson, N. (2011) Uncertainty, emergence, and statistics in dendrochronology. *Dendroclimatology* (ed. by M.K. Hughes, T.W. Swetnam and H.F. Diaz), pp. 77–112. Developments in Paleoenvironmental Research, Volume 11. Springer Science + Business Media, Dordrecht, The Netherlands.

Cook, E.R. & Peters, K. (1997) Calculating unbiased tree-ring indices for the study of climatic and environmental change. *The Holocene*, **7**, 361–370.

Cook, E.R., Glitzenstein, J.S., Krusic, P.J. & Harcombe, P.A. (2001) Identifying functional groups of trees in West Gulf Coast forests (USA): a tree-ring approach. *Ecological Applications*, **11**, 883–903.

Cook, E.R., Anchukaitis, K., Buckley, B., D'Arrigo, R., Jacoby, G. & Wright, W. (2010) Asian monsoon failure and megadrought during the last millennium. *Science*, **328**, 486–489.

Esper, J., Cook, E.R. & Schweingruber, F.H. (2002) Low-frequency signals in long tree-ring chronologies for reconstructing past temperature variability. *Science*, **295**, 2250–2253.

Esper, J., Niederer, R., Bebi, P. & Frank, D.C. (2008) Climate signal age effects – evidence from young and old trees in the Swiss Engadin. *Forest Ecology and Management*, **255**, 3783–3789.

Frank, D.C. & Esper, J. (2005) Temperature reconstructions and comparisons with instrumental data from a tree-ring network for the European Alps. *International Journal of Climatology*, **25**, 1437–1454.

Frank, D.C., Esper, J. & Cook, E.R. (2007) Adjustment for proxy number and coherence in a large-scale temperature reconstruction. *Geophysical Research Letters*, **34**, L16709.

Frank, D.C., Esper, J., Raible, C., Büntgen, U., Trouet, V., Stocker, B. & Joos, F. (2010) Ensemble reconstruction constraints on the global carbon cycle sensitivity to climate. *Nature*, **463**, 527–530.

Friedlingstein, P., Houghton, R.A., Marland, G., Hackler, J., Boden, T.A., Conway, T.J., Canadell, J.G., Raupach, M.R.,

Ciais, P. & Le Quéré, C. (2010) Update on CO_2 emissions. *Nature Geoscience*, **3**, 811–812.

Friedrichs, D.A., Trouet, V., Büntgen, U., Frank, D.C., Esper, J., Neuwirth, B. & Löffler, J. (2009) Species-specific climate sensitivity of tree growth in central-west Germany. *Trees – Structure and Function*, **23**, 729–739.

Fritts, H.C. (1976) *Tree rings and climate*. The Blackburn Press, Caldwell.

Gouirand, I., Linderholm, H., Moberg, A. & Wohlfarth, B. (2008) On the spatiotemporal characteristics of Fennoscandian tree-ring based summer temperature reconstructions. *Theoretical and Applied Climatology*, **91**, 1–25.

Helama, S., Lindholm, M., Meriläinen, J., Timonen, M. & Eronen, M. (2005) Multicentennial ring-width chronologies of Scots pine along a north–south gradient across Finland. *Tree-Ring Research*, **61**, 21–32.

Hewitson, B.C. & Crane, R.G. (2002) Self-organizing maps: applications to synoptic climatology. *Climate Research*, **22**, 13–26.

Hickler, T., Vohland, K., Feehan, J., Miller, P.A., Smith, B., Costa, L., Giesecke, T., Fronzek, S., Carter, T.R., Cramer, W., Kühn, I. & Sykes, M.T. (2012) Projecting the future distribution of European potential natural vegetation zones with a generalized, tree species-based dynamic vegetation model. *Global Ecology and Biogeography*, **21**, 50–63.

Hijmans, R.J., Cameron, S.E., Parra, J.L., Jones, P.G. & Jarvis, A. (2005) Very high resolution interpolated climate surfaces for global land areas. *International Journal of Climatology*, **25**, 1965–1978.

Hoch, G. & Körner, C. (2012) Global patterns of mobile carbon stores in trees at the high-elevation tree line. *Global Ecology and Biogeography*, **21**, 861–871.

Jolly, W., Dobbertin, M., Zimmermann, N. & Reichstein, M. (2005) Divergent vegetation growth responses to the 2003 heat wave in the Swiss Alps. *Geophysical Research Letters*, **32**, L18409.

Jung, M., LeMaire, G., Zaehle, S., Luyssaert, S., Vetter, M., Churkina, G., Ciais, P., Viovy, N. & Reichstein, M. (2007) Assessing the ability of three land ecosystem models to simulate gross carbon uptake of forests from boreal to Mediterranean climate in Europe. *Biogeosciences*, **4**, 647–656.

Levanic, T., Gricar, J., Gagen, M., Jalkanen, R., Loader, N.J., McCarroll, D., Oven, P. & Robertson, I. (2009) The climate sensitivity of Norway spruce (*Picea abies* (L.) Karst.) in the southeastern European Alps. *Trees – Structure and Function*, **23**, 169–180.

Luyssaert, S., Ciais, P., Piao, S.L. *et al.* & Members of the Carboeurope-Ip Synthesis Team (2010) The European carbon balance. Part 3: forests. *Global Change Biology*, **16**, 1429–1450.

McDowell, N., Beerling, D., Breshears, D., Fisher, R., Raffa, K. & Stitt, M. (2011) The interdependence of mechanisms underlying climate-driven vegetation mortality. *Trends in Ecology and Evolution*, **26**, 523–532.

Metsaranta, J. & Kurz, W.A. (2012) Inter-annual variability of ecosystem production in boreal jack pine forests (1975–2004) estimated from tree-ring data using CBM-CFS3. *Ecological Modelling*, **224**, 111–123.

Metsaranta, J. & Lieffers, V. (2009) Using dendrochronology to obtain annual data for modelling stand development: a supplement to permanent sample plots. *Forestry*, **82**, 163–173.

Mitchell, C.D. & Jones, P. (2005) An improved method of constructing a database of monthly climate observations and associated high-resolution grids. *International Journal of Climatology*, **25**, 693–712.

Moser, L., Fonti, P., Büntgen, U., Esper, J., Luterbacher, J., Franzen, J. & Frank, D. (2010) Timing and duration of European larch growing season along altitudinal gradients in the Swiss Alps. *Tree Physiology*, **30**, 225–233.

Neuwirth, B., Esper, J., Schweingruber, F.H. & Winiger, M. (2004) Site ecological differences to the climatic forcing of spruce pointer years from the Lötschental, Switzerland. *Dendrochronologia*, **21**, 69–78.

Nicault, A., Alleaume, S., Brewer, S., Carrer, M., Nola, P. & Guiot, J. (2008) Mediterranean drought fluctuation during the last 500 years based on tree-ring data. *Climate Dynamics*, **31**, 227–245.

Pan, Y., Birdsey, R.A., Fang, J., Houghton, R., Kauppi, P.E., Kurz, W.A., Phillips, O.L., Shvidenko, A., Lewis, S.L., Canadell, J.G., Ciais, P., Jackson, R.B., Pacala, S., McGuire, A.D., Piao, S., Rautiainen, A., Sitch, S. & Hayes, D. (2011) A large and persistent carbon sink in the world's forests. *Science*, **333**, 988–993.

Panayotov, M., Bebi, P., Trouet, V. & Yurukov, S. (2010) Climate signal in tree-ring chronologies of *Pinus peuce* and *Pinus heldreichii* from the Pirin Mountains in Bulgaria. *Trees – Structure and Function*, **24**, 479–490.

Piao, S.L., Ciais, P., Friedlingstein, P., Noblet-Ducoudre, N., Cadule, P., Viovy, N. & Wang, T. (2009) Spatiotemporal patterns of terrestrial carbon cycle during the 20th century. *Global Biogeochemical Cycles*, **23**, GB4026.

Poulter, B., Frank, D.C., Hodson, E.L. & Zimmermann, N.E. (2011) Impacts of land cover and climate data selection on understanding terrestrial carbon dynamics and the CO_2 airborne fraction. *Biogeosciences*, **8**, 2027–2036.

Sitch, S., Huntingford, C., Gedney, N., Levy, P.E., Lomas, M., Piao, S.L., Betts, R., Ciais, P., Cox, P., Friedlingstein, P., Jones, C.D., Prentice, I.C. & Woodward, F.I. (2008) Evaluation of the terrestrial carbon cycle, future plant geography and climate-carbon cycle feedbacks using five dynamic global vegetation models (DGVMs). *Global Change Biology*, **14**, 2015–2039.

St George, S., Meko, D.M. & Cook, E.R. (2010) The seasonality of precipitation signals embedded within the North American Drought Atlas. *Holocene*, **20**, 983–988.

Stegen, J.C., Swenson, N.G., Enquist, B.J., White, E.P., Phillips, O.L., Jørgensen, P.M., Weiser, M.D., Monteagudo Mendoza, A. & Núñez Vargas, P. (2011) Variation in above-ground forest biomass across broad climatic gradients. *Global Ecology and Biogeography*, **20**, 744–754.

Tegel, W., Vanmoerkerke, J. & Büntgen, U. (2010) Updating historical tree-ring records for climate reconstruction. *Quaternary Science Reviews*, **29**, 1957–1959.

Trouet, V., Taylor, A.H., Carleton, A.M. & Skinner, C.N. (2006) Fire–climate interactions in forests of the American Pacific coast. *Geophysical Research Letters*, **33**, L18704.

Van der Maaten-Theunissen, M. & Bouriaud, O. (2012) Climate–growth relationships at different stem heights in silver fir and Norway spruce. *Canadian Journal of Forest Research*, **42**, 958–969.

Van der Schrier, G., Briffa, K.R., Jones, P.D. & Osborn, T.J. (2006) Summer moisture variability across Europe. *Journal of Climate*, **19**, 2818–2834.

Wettstein, J., Littell, J., Wallace, J. & Gedalof, Z. (2011) Coherent region, species and freqency-dependent local climate signals in Northern Hemisphere tree-ring widths. *Journal of Climate*, **24**, 5998–6012.

Wigley, T.M.L., Briffa, K.R. & Jones, P.D. (1984) On the average value of correlated time series, with applications in dendroclimatology and hydrometeorology. *Journal of Climate and Applied Meteorology*, **23**, 201–213.

Wilson, R., Loader, N., Rydval, M., Paton, H., Frith, A., Mills, C., Crone, A., Edwards, C., Larsson, L. & Gunnarson, B. (2012) Reconstructing Holocene climate from tree rings – the potential for a long chronology from the Scottish Highlands. *The Holocene*, **22**, 3–11.

Zhao, M. & Running, S. (2010) Drought-induced reduction in global terrestrial net primary production from 2000 through 2009. *Science*, **329**, 940–943.

Zobler, L. (1986) *A world soil file for global climate modelling.* NASA Technical Memorandum. NASA Goddard Institute for Space Studies, New York.

Zweifel, R., Eugster, W., Etzold, S., Dobbertin, M., Buchmann, N. & Häsler, R. (2010) Link between continuous stem radius changes and net ecosystem productivity of a subalpine Norway spruce forest in the Swiss Alps. *New Phytologist*, **187**, 819–830.

SUPPORTING INFORMATION

Additional supporting information may be found in the online version of this article at the publisher's web-site.

Appendix S1 Dynamic global vegetation model description.
Appendix S2 Supplementary figures.
Appendix S3 Readme datafiles.
Appendix S4 Tree-ring network.
Appendix S5 Monthly net primary production ORCHIDEE-FM.
Appendix S6 Monthly net primary production LPJ-wsl.

BIOSKETCH

Flurin Babst's research interests include large-scale (i.e. continental to global) interactions of climate variability and forest growth. Particular emphasis is placed on using dendroclimatological/dendroecological methods to reconstruct past growth dynamics at annual resolution. Flurin Babst's research activities contribute to reducing uncertainties in the terrestrial carbon cycle's response to abiotic (e.g. climate extremes) and biotic (e.g. insect outbreaks) forcing agents.

Editor: Martin Sykes